RSC Advances

ROYAL SOCIETY OF CHEMISTRY

www.rsc.org/advances

Journal Name

ARTICLE

Phase Purification of Cu-S System towards $Cu_{1.8}S$ and its Catalytic Properties for a Clock Reaction

Received 00th January 2015,
Accepted 00th January 2015

DOI: 10.1039/x0xx00000x

www.rsc.org/

Yuanjun Liu,[a] Guoxing Zhu,[b, c, *] Jing Yang,[b] Chunlin Bao,[b] Jing Wang,[a] Aihua Yuan[a,*]

Controlling the composition and crystal phase is an important issue to tune material physical/chemical properties. Herein, it was found that triphenyl phosphine (TPP) can be used as a phase transfer agent to transform CuS, $Cu_{39}S_{28}$ phases into pure low-sulfur $Cu_{1.8}S$ phase. When mixed phase copper sulfides were reacted with triphenyl phosphine under suitable temperature, sulfur was extracted to produce the low-sulfur $Cu_{1.8}S$ phase. It was also demonstrated that the Cu-S product can effectively catalyze a clock reaction between methylene blue and hydrazine in aqueous medium. In addition, the photothermal conversion properties of the Cu-S based products were studied. The results show that the purified $Cu_{1.8}S$ materials show enhanced or similar properties than the original mixed-phase Cu-S products.

Introduction

Metal chalcogenide semiconductor materials have been intensively studied in recent years out of scientific interest and because of their wide technological application.[1-3] Their physical and chemical properties can be highly modified by minute changes in their microscale morphology and size. Besides morphology and size, chemical composition and crystal phase are another two basic parameters for tuning their physical or chemical properties through influencing the bonding characteristic, vacancies, and so on.[4-5] For examples, careful tuning the oxygen stoichiometry in copper oxide materials can induce the transferring of various superconducting, electronic, and magnetic states.[6] FeSe at a very precise composition in window of 50.6-51.0% Fe is superconducting, while NiAs-type FeSe with a nominally 1:1 of Fe to Se (42.0-50.5%) is not superconducting.[7] Hence, precise controlling and modulating the composition or crystal phase of metal chalcogenide materials is of large scientific and technological importance.

The electrical conductivity breadth from metallic to semiconducting to superconducting and the defect chemistry owing to nonstoichiometry for copper sulfides render them attractive for various applications.[8-22] Copper sulfides with various Cu/S ratios have demonstrated great potential for wide applications in fields such as solar cells, photoelectric transformers, nano-switches, thermoelectric materials, electrocatalysts and photocatalysts.[23-24] The Cu-S system has at least nine kinds of different crystal phase with the varied x value in $Cu_{2-x}S$ (x= 0-1) including Cu_2S (γ- and β-chalcocite),[25] $Cu_{1.98}S$ (djurleite),[26] $Cu_{1.8}S$ (digenite),[27, 28] $Cu_{1.75}S$ (anilite),[29, 30] and CuS (covellite), [31, 32] as shown in the X-ray diffraction pattern database. The energy band structure and physical/chemical properties of $Cu_{2-x}S$ are highly dependent on the stoichiometric factor, *2-x*. However, it is not always straightforward for synthesizing a copper sulfide product with targeting phase; usually, mixed phase copper sulfide products are often obtained through usual synthesis strategies. Up to date, some methods including phase transformation route have been devoted for the preparation of copper sulfide products with pure specific phase.[26, 33-35] For example, it was demonstrated that Cu_7S_4 and CuS can be obtained from the freshly formed Cu_9S_8 nanocrystals.[36] With a solid-state annealing route, CuS also undergoes a reduction to tetragonal cuprous sulfide Cu_2S.[37] Recently, Fang *et al* reported facile synthesis of $Cu_{39}S_{28}$ microcrystals *via* a solvothermal route.[38] Alivisatos *et al* has demonstrated the temperature-induced structural trans-formations of Cu_2S nanorods from a low to a high chalcocite structure and investigated their size dependent phase transformation behaviour.[39, 40] Zhong *et al* reported a phase transformation process from rhombohedral $Cu_{1.8}S$ nanocrystals to hexagonal CuS clusters.[41] In spite of these valuable investigations, relative to highly studied PbS and CdS micro-/nanoscale materials, copper sulfides have not been extensively studied. In addition, as copper sulfide easily forms different but close stoichiometric phases, controlling of copper sulfide crystal phase with simple method is still a challenge.[42-44]

Among the various $Cu_{2-x}S$ materials, $Cu_{1.8}S$, which is a useful *p*-type semiconductor with indirect bandgap of 1.5-1.6 eV, has got much attention due to its rich properties and potential applications.[14, 40, 45, 46] $Cu_{1.8}S$ is known to be used as thermo- or photoelectric transformers and high-temperature

[a] School of Environmental and Chemical Engineering, Jiangsu University of Science and Technology, Zhenjiang 212018, China. Email: aihuayuan@just.edu.cn
[b] School of Chemistry and Chemical Engineering, Jiangsu University, Zhenjiang, 212013, China, Email: zhuguoxing@ujs.edu.cn
[c] State Key Laboratory of Coordination Chemistry, Nanjing University, Nanjing, 210093, China

thermistors. The higher copper deficiency in $Cu_{1.8}S$ material makes it show unique localized surface plasmon resonance effect (LSPR).[40] Due to the LSPR effect, $Cu_{1.8}S$ has shown excellent photothermal conversion effect and would be used as new type of photothermal agent.[45-46] Especially, it was also demonstrated that $Cu_{1.8}S$ with higher ion deficiency can be used as catalyst inducing the formation of heterostructures.[14]

In this study, a simple and low cost hydrothermal method was developed for the synthesis of copper sulfide product. The obtained product contains two kinds of copper sulfides (CuS and $Cu_{1.8}S$). Based on this, we described a new chemical extraction route with triphenyl phosphine (TPP) as extraction agent. This extraction process can transform CuS, $Cu_{39}S_{28}$ phases into pure low-sulfur metastable rhombohedral phase $Cu_{1.8}S$. This chemistry has at least three important implications. First, sulfur-rich copper sulfides can be chemically transformed into $Cu_{1.8}S$ phase *via* TPP extraction of sulfur. This highlights the possibility of precise $Cu_{1.8}S$ phase targeting with this route. Secondly, impure samples contain mixtures of multiple copper sulfides including CuS, $Cu_{1.8}S$, $Cu_{39}S_{28}$ can be purified by TPP extraction of sulfur, with the final product exclusively being metastable rhombohedral $Cu_{1.8}S$ phase. Third, it seems that the $Cu_{1.8}S$ product obtained with purification route shows similar properties to that of $Cu_{1.8}S$ sample obtained with direct preparation route.

Experimental

Materials

$CuCl_2 \cdot 2H_2O$, thiourea, polyvinylpyrrolidone (PVP, K30, Mw = 58000), ethylene glycol, triphenylphosphine, N, N-dimethyl-formamide (DMF), chloroform, and ethanol employed in this research were analytical grade and used without further purification. Deionized water was used in the experiments.

Synthesis of mixed-phase copper sulfide products

In a typical synthesis, 1.36 mmol of $CuCl_2 \cdot 2H_2O$, 1.85 mmol of thiourea, and 0.2 g of PVP (K-30) were dissolved in 18 mL of ethylene glycol to obtain a clear solution. The solution was then transferred into a 30 mL of Teflon-lined autoclave, sealed and heated at 180 ^oC for 12 h and then cooled down to room temperature naturally. The final products were collected by centrifugation and washed with deionized water and absolute ethanol for several times. The as-obtained products were then dried in a 45 ^oC vacuum oven for further characterization. The sample contains mixed phase copper sulfides, CuS and $Cu_{1.8}S$.

Synthesis of $Cu_{39}S_{28}$ phase copper sulfide

$Cu_{39}S_{28}$ phase sample was prepared according to a reported method.[38] In a typical synthesis, 2 mmol of $Cu(NO_3)_2 \cdot 3H_2O$, 2 mmol of thiourea, and 2.0 g of PVP were absolutely dissolved in 20 mL of DMF. The obtained system was then stirred for about 30 min to obtain a clear green solution, which was then transferred into a 30 mL Teflon-lined stainless steel autoclave, sealed and heated at 120 ^oC for 12 h. After cooling down to room temperature naturally, the obtained $Cu_{39}S_{28}$ product was collected by centrifugation, washed with distilled water and absolute ethanol, and dried at 45 ^oC under vacuum.

Phase transformation of copper sulfides to $Cu_{1.8}S$ phase

Typically, 5 g of TPP was heated to 100 ^oC in a 50 mL of three-necked flask and was kept at this temperature for 15 min with stirring. 30 mg of copper sulfide sample (mixture of CuS and $Cu_{1.8}S$, or $Cu_{39}S_{28}$) was then added. After reaction at 100 ^oC for 2 h, the product was collected by centrifugation, washed with chloroform and ethanol for several times, and dried at 45 ^oC under vacuum.

Characterization

XRD patterns were recorded on an X-ray diffractometer (Bruker D8 Advance diffractometer) with Cu Kα radiation (λ = 1.5406 Å) at a scanning rate of 5° min^{-1}. Ultraviolet-visible (UV-vis) spectroscopy measurements were performed on a UV-2450 ultraviolet-visible spectrophotometer. The morphology and micostructure analyses were conducted on Hitachi S-4800 field emission scanning electron microscope (SEM) and a JEM-2010 transmission electron microscope (TEM).

Catalytic properties

In a typical reaction, 100 μL (~1×10^{-5} mol/L, about 17 μg/mL) of copper sulfide aqueous dispersion was mixed with an 200 μL of methylene blue (MB) aqueous solution (with concentration of 5×10^{-4} mol/L) in a 1 cm quartz cuvette, and the volume of the reaction system was added up to 3 mL with deionized water. 100 μL of 2.5 M aqueous hydrazine hydrate solution was then added to the reaction mixture to induce the reaction. After addition of hydrazine hydrate solution, the blue color of MB gradually disappeared. The reaction mixture regained its original blue shade just shaking the mixture in air for several seconds. For detecting the color change of the reaction system, time-dependent absorption spectra were recorded with a UV-visible spectrophotometer at room temperature.

Measurement of photothermal conversion effect of the copper sulfide materials

For measuring temperature change due to the photothermal conversion effect of copper sulfide materials, 980 nm near infrared (NIR) laser was delivered through a quartz glass cuvette containing aqueous dispersion (1 mL with concentration of 0.03 mg/mL) of copper sulfide samples with magnetic stirring. The light source is 0.5 W with a laser beam diameter of 6 mm (Ningbo Ruanming Laser Technology Co., Ltd. China). A thermocouple with an accuracy of 0.5 ^oC was inserted into the aqueous dispersion of the tested samples for recording the change of real-time temperature. The temperature was recorded one time per 20 s.

Results and discussion

Synthesis and Characterization

In our study, TPP was used as the crystal-phase transform agent. TPP is usually used as nanoparticle capping agent owing t o

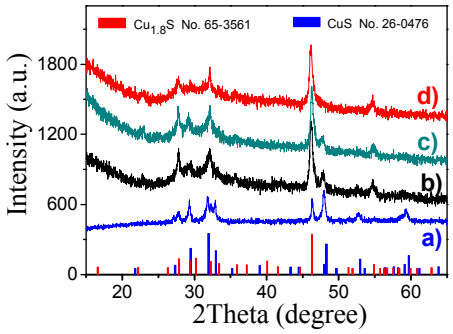

Fig. 1 XRD patterns of a) the synthesized mixed phase sample containing CuS and $Cu_{1.8}S$ and the products after treated by TPP for b) 0.5 h, c) 1 h, and d) 2h at 100 °C. The standard JCPDS XRD patterns for CuS (No. 65-3561) and $Cu_{1.8}S$ (No. 26-0476) are also shown in the bottom.

its strong coordination ability of phosphorus atom, phosphorous source for chemical synthesis. Especially, it is also used as a chemical agent in the form of TPP-S complexes. The phase transform process is simple. Direct heating of the copper sulfide dispersion in TPP will induce the phase transform of copper sulfides. Figure 1 shows the powder X-ray diffraction (XRD) data for the purification process. It is clear that the original Cu-S products contain two kinds of copper sulfide phase, hexagonal covellite CuS (JCPDS No. 65-3561) and rhombohedral digenite $Cu_{1.8}S$ (JCPDS No. 26-0476). After treated with TPP at 100 °C for 0.5 h, the XRD diffraction peaks corresponding to hexagonal CuS decrease, suggesting the transform process of CuS to $Cu_{1.8}S$ is conducted. With 2 h of treatment, the obvious enhancement of the peaks at about 2θ = 46.2, 54.8°, and the absolute disappearing of the peak at about 2θ = 47.9° indicate that pure phase $Cu_{1.8}S$ is obtained after this treatment. This result suggests that TPP can successfully extract sulfer from sulfur-rich copper sulfide, CuS, forming the corresponding low-sulfur compound, $Cu_{1.8}S$ phase.

We also investigate the morphology change of the copper

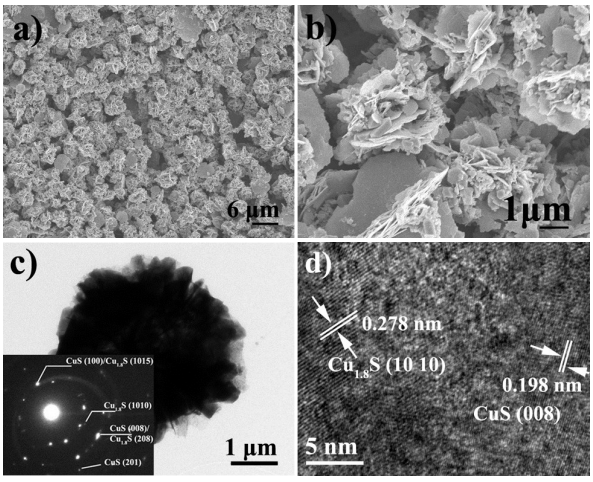

Fig. 2 a, b) SEM, c) TEM, and d) HRTEM images of the mixed phase copper sulfides. Inset of c) shows the SAED pattern of the product.

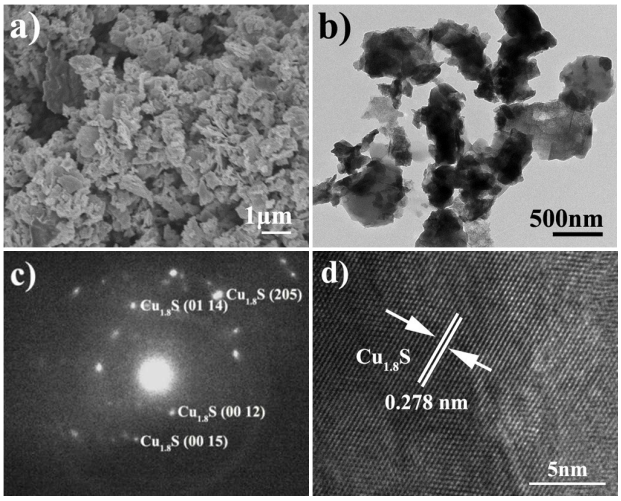

Fig. 3 a) SEM, b) TEM, c) SAED pattern, and d) HRTEM images of the purified $Cu_{1.8}S$ product.

sulfide products during the phase transformation process. Figure 2 shows the SEM and TEM images of the mixture phase copper sulfides. It can be seen that the original mixture phase copper sulfide product is composed of flower-like micro-spheres with size of 3-5 μm (Figure 2a, b). The flower-like microspheres are assembled by sheet-like units. Some irregular particles are loaded on the flower-like microstructure, suggesting the mixture phase. TEM image shows similar results (Figure 2c). Inset of Figure 2c shows the selected area electron diffraction pattern (SAED). The pattern can be indexed into CuS and $Cu_{1.8}S$, although they have similar crystal plane spacing. Two kinds of clear lattice fringes with different spacing in the high-resolution TEM indicate the high crystallinity and two different crystal phases involved in it (Figure 2d). The lattice fringe with spacing of 0.278 nm would be indexed to (10 10) plane of $Cu_{1.8}S$, while that of 0.198 nm can be attributed to (008) plane of CuS. After phase purification with TPP, the morphology of the copper sulfide changed. The assembled flower-like microspheres are broken, leaving disorder sheet-like units (Figure 3a, b). The corresponding SAED pattern and HRTEM shows pure $Cu_{1.8}S$ phase with high crystallinity (Figure 3c, d). The morphology change indicates the chemical reaction between copper sulfide and TPP.

It was found that the formation of $Cu_{1.8}S$ phase by TPP treatment is highly phase-targeting. Increasing the treatment temperature to 200 °C, the obtained product is still $Cu_{1.8}S$ phase. Interestingly, other copper sulfide phase, for example $Cu_{39}S_{28}$, can also be transferred into the rhombohedral $Cu_{1.8}S$ phase by this phase transform route. The corresponding results are shown in Figure 4. $Cu_{39}S_{28}$ sample was synthesized according to a reported method. Although the XRD patterns are difficult to distinguish owing to the relatively weak crystalline and the close XRD patterns between $Cu_{39}S_{28}$ and $Cu_{1.8}S$ phase, after TPP treatment, an obvious shift of the strongest peak is clearly observed, suggesting the crystal phase transformation.

These results suggest that TPP can extract sulfur from sulfur-rich copper sulfide, forming metal-rich $Cu_{1.8}S$ phase.

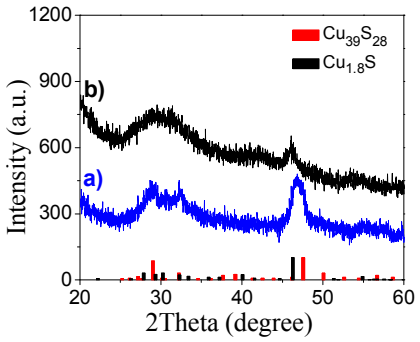

Fig. 4 XRD patterns of a) the synthesized $Cu_{39}S_{28}$ product and b) that after treated by TPP for 2 h at 100 °C. The standard JCPDS XRD patterns for $Cu_{39}S_{28}$ (No. 36-0380) and $Cu_{1.8}S$ (No. 26-0476) are shown in the bottom.

This extract process is quite different from the previous reported Cu(I) induced phase transformation route.[43] In that case, Cu(I) specie was found to induce $Cu_{1.1}S$ phase to $Cu_{1.1\text{-}1.5}S$ phase. It was proposed that a fraction of Cu^+ ions from the solution enters the $Cu_{1.1}S$ lattice, matched by a transfer of electrons from the solution. In our route, it seems that TPP extract sulfur from sulfur-rich covellite CuS product, causing the phase transformation. There are reports about crystal structure of hexagonal covellite CuS.[47-50] Studies have shown that the valence of copper in covellite CuS is monovalent with formalism of $(Cu^+)_3(S_2^{2-})(S^-)$ or $(Cu^+)_3(S_2^-)(S^{2-})$.[43, 47] Recent experiments and calculations have put the valence of Cu between 1 and 1.5 (1.33 for CuS from calculations).[50] While, all studies indicate that sulfur in covellite phase exists with various valence or forms. Figure 5 shows the crystal structure illustration of covellite CuS phase and digenite $Cu_{1.8}S$. From the structural point of view, it is important to note the similarities of the Cu or S sub-lattice between covellite and digenite in the corresponding close-packed planes, *i.e.* (001) and (10-1), respectively. It would make it easily to transfer covellite CuS to digenite $Cu_{1.8}S$ under suitable reaction conditions.

In our case, the extract route is possibly driven by the large formation constant of the TPP-S complexes. The bonding of sulfur and TPP would be stronger, which cause the following reaction proceed.

$$CuS + TPP \rightarrow Cu_{1.8}S + TPP\text{-}S$$

In the phase transformation process, solid copper sulfide reacts with liquid TPP causing the phase transformation. Thus the reaction rate would be controlled by the solid-liquid interface reaction.

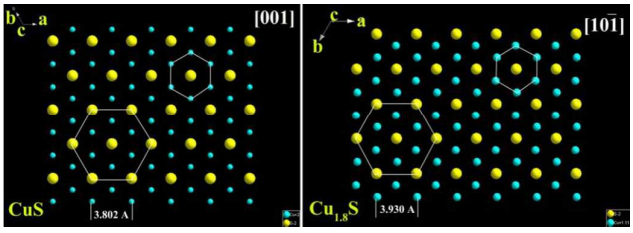

Fig. 5 Crystal structure illustration of covellite CuS and digenite $Cu_{1.8}S$.

Catalytic properties

It is known that nanoscale copper-based compounds have very good catalytic performance.[51, 52] To investigate the catalytic properties of $Cu_{1.8}S$ products obtained from the purified procedure, the reaction between methylene blue (MB) and hydrazine in aqueous medium was conducted. The reaction shows quite slow reaction rate if no any catalysts were involved. With suitable catalysts, chemical oscillation phenomenon between blue color MB and colorless leucomethylene blue (LMB) can be observed with periodic shaking. Although it was reported that some copper-based materials can effectively catalyze this reaction, CuO or Cu nanoparticles did not show any catalytic effect for it.[51, 53]

In the presence of copper sulfide catalyst, hydrazine will gradually reduce MB at room temperature, forming colorless LMO (as shown above reaction scheme 1). While, upon further

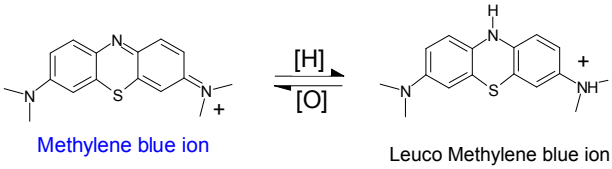

Scheme 1. The chemical oscillation reaction based on methylene blue ions.

shaking reaction system in air, the colorless LMO will be oxidized again by air forming blue MB. The redox process demonstrates a simple "clock reaction", which provides an engaging illustration of redox phenomena and reaction kinetics. As shown in Figure 6, the original blue reaction solution gradually becomes weak with the increasing of duration time. With duration time of about 20 min, only the liquid-air interface shows blue color, while the solution body becomes colorless. This is reasonable since oxygen in air will oxidize LMO. Further prolonging the duration time to 3 h, the air in the sealed system is possibly exhausted, so the whole solution is colorless. Once shaking the reaction system in air, blue color quickly reappears.

Based on the fact that MB exhibits an intense absorption band in the region of 500-700 nm and LMB shows no

Fig 6. Schematic representation of the "clock reaction" catalyzed by $Cu_{1.8}S$, that is, blue color fading and regeneration of MB.

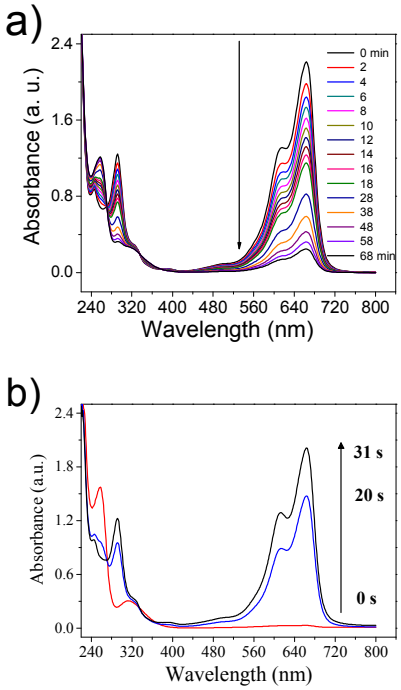

Fig 7. a) Absorption spectra for successive decolorization of MB and b) colour regeneration catalyzed by $Cu_{1.8}S$.

absorption at this region, we monitored the process of the clock reaction by a UV-visible spectrophotometer. With the MB blue color bleaching, a steady decrease of the absorbance of MB was measured at same intervals, as shown in Figure 7a. It should be noted that in the absence of copper sulfide catalyst, no such a decrease in the absorbance of MB was observed in the same experimental condition. Thus, the important role of the synthesized copper sulfide product in the "clock reaction" is no doubt concluded.

It seems that the synthesized $Cu_{1.8}S$ product has a strong catalytic ability for the reduction of MB by hydrazine at room temperature. We also investigated the catalytic activities of mixed phase copper sulfides and $Cu_{39}S_{28}$ product. In contrast, the catalytic activities of them are relatively low (Figure SI-1, SI-2, see Supporting Information). After complete reduction of MB, the solution containing colourless LMB can again regenerate the blue color in the presence of small amount aerial O_2 on shaking of the reaction mixture openly and so the characteristic absorption band appears (shown in Figure 7b).

We then investigated the influence of various experimental parameters on the reaction kinetics. It was found that without hydrazine, the reaction cannot proceed. More hydrazine is involved, the reaction rate is quickly. While, it seems that the catalyst dosage don't have obvious influence on the reaction rate in our investigated range. In the presence of copper sulfide catalysts, the plot of absorption factor as a function of time (Figure 8a) shows a profile of exponential equation, $A_t = A_0e^{-kt}$, which is consistent with a pseudo-first-order reaction. Thus, pseudo-first-order reaction kinetics was applied for the evaluation of catalytic activity in our case. The relation of $\ln(A_t/A_0)$ (at peak of 664 nm) versus time is shown in Figure 8b. The slope of the straight line gives the rate constant of the catalytic reaction, 0.0323 min^{-1} for pure $Cu_{1.8}S$. While, mixed phase copper sulfide sample shows similar and relatively lower rate constant, 0.0297 min^{-1}. This indicates that the purified procedure don't change the catalytic activity of the copper sulfide product. In addition, the $Cu_{39}S_{28}$ product shows the poorest catalytic activity among the tested three samples. It is proposed that the tiny composition difference and the different crystal phase cause their different properties. Copper sulfides with different phases have different copper and sulfur ions arrangement in the crystal, which will cause the different chemical surroundings for the copper or sulfur ions. This finally induces the different catalytic or related properties.

We then proposed a possible catalytic principle for the reaction. It is proposed that copper sulfide would promote the electron transfer process from hydrazine to MB.[51] During the reaction, hydrazine and MB may be absorbed onto the copper sulfide surface due to the reasonable affinity. It is believed that hydrazine supplies electrons to MB via copper sulfide, causing the generation of colorless LMB. Hydrazine transfers electrons to Cu(I) to reduce it to Cu(0). Then, MB and dissolved oxygen in the system oxidizes Cu(0) back to Cu(I).[51] During this process, MB was reduced forming colorless LMB. The electron-transfer processes can be supported by the redox potential values of $\varphi(N_2/N_2H_4)$ = -1.16 V, $\varphi(Cu^+/Cu)$ = 0.52 V, φ(MB/LMB) = 1.08 V.[51, 54] In the reaction system, excess hydrazine in turn decreases the dissolved oxygen concentration in water, which facilitates LMB formation. While, indeed, detailed catalytic mechanism needs further study.

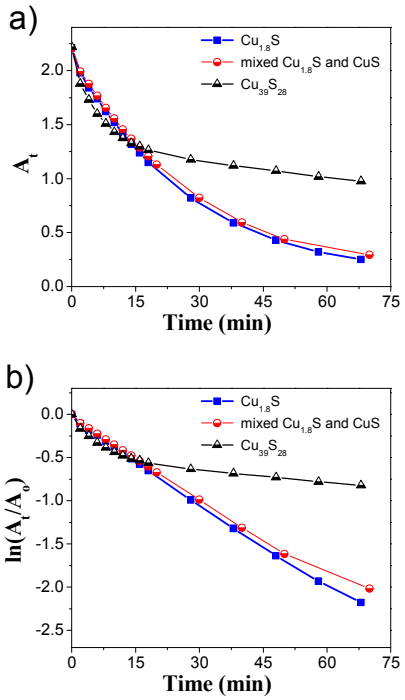

Fig 8. Plots of a) A_t and b) $\ln(A_t/A_o)$ of MB *vs* reaction time in the presence of mixed copper sulfides, $Cu_{39}S_{28}$, and pure $Cu_{1.8}S$.

In addition, it is recently reported that Cu-S system is a new promising semiconductor photothermal conversion platforms with relatively high photothermal conversion efficiency, good photostability, synthetic simplicity, low toxicity and low cost.[42] It can effectively induce temperature elevation under NIR irradiation, which would provide a possible route for cancer treatment.

The NIR photothermal conversion property of the obtained Cu-S samples in the aqueous dispersions was then examined at a fixed concentration of 0.03 mg/mL. The results are shown in Figure 9. The pure water system was also tested for comparison. It is obvious that, for the pure water, the NIR irradiation (980 nm) caused a temperature increase of only about 4 °C after 8 min. For the aqueous dispersion of Cu-S products, the NIR irradiation induced temperature elevation is much higher than the pure water. For the mixtured sample with CuS and $Cu_{1.8}S$ phase, the temperature increase is 6 °C, while the pure phase $Cu_{1.8}S$ sample gives a higher temperature increase of 7 °C, suggesting the better photothermal conversion property of $Cu_{1.8}S$ than that of CuS. It should be noted that all the aqueous dispersions reach a temperature platform with irradiation for 8 min, suggesting a thermal equilibrium between laser energy input and thermal diffusion towards environment are obtained at this stage. After that, the laser is closed, the temperature then decreases to room temperature.

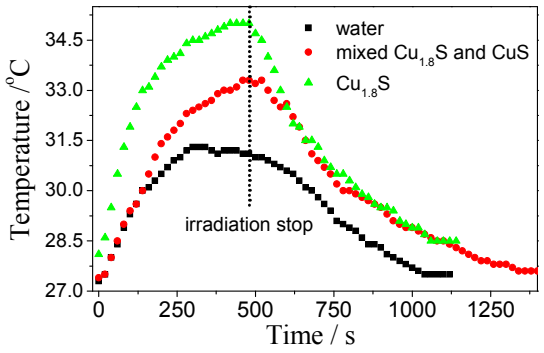

Fig 9. Temperature variations for pure water and aqueous dispersions of the obtained copper sulfide samples with NIR irradiation time for 0-8 min, and then the laser was shut off. The concentration of the Cu-S products is 0.03 mg/mL.

Conclusions

We have demonstrated that TPP can be used for the phase-selective extraction of sulfur from sulfur-rich copper sulfides. This provides a new phase transformation strategy for manipulating the compositions and structures of Cu-S system, which would also have applicability to purification of multiphase samples. In addition, the clock reaction catalyzed by Cu-S based product has been demonstrated. Our study on the catalytic properties and the photothermal conversion properties of the Cu-S based products reveals that the obtained $Cu_{1.8}S$ materials show enhanced or similar properties than the original mixed-phase Cu-S products.

Acknowledgements

The authors are grateful for financial support from National Natural Science Foundation of China (No. 51203069, 51102117, 21201010, 21203079), Jiangsu Natural Science Foundation (No. BK2012276), and Cultivating Project of Young Academic Leader from Jiangsu University.

Notes and references

1 N. P. Dasgupta, X. B. Meng, J. W. Elam and A. B. F. Martinson, *Acc. Chem. Res.*, 2015, **48**, 341-348.
2 P. Miro, M. Audiffred and T. Heine, *Chem. Soc. Rev.*, 2014, **43**, 6537-6554.
3 X. F. Duan, Y. Huang, R. Agarwal and C. M. Lieber, *Nature*, 2001, **421**, 214-245.
4 S. M. Farkhani and A. Valizadeh, *Let Nanobiotechnol.*, 2014, **8**, 59-76.
5 Q. Li, B. D. Guo, J. G. Yu, J. R. Ran, B. H. Zhang, H. J. Yan and J. R. Gong, *J. Am. Chem. Soc.*, 2011, **133**, 10878-10884.
6 M. Karppinen and H. Yamauchi, *Mater. Sci. Eng.*, 1999, **26**, 51-96.
7 T. M. Mcqueen, Q. Huang, V. Ksenofontov, C. Felser, Q. Xu, H. Zandbergen, Y. S. Hor, J. Allred, A. J. Williams, D. Qu, J. Checkelsky, N. P. Ong and R. J. Cava, *Phys. Rev. B*, 2009, **79**, 014522-1-7.
8 T. A. Miller, J. S. Wittenberg, H. Wen, S. Connor, Y. Cui and A. M. Lindenberg, *Nat. Commun.*, 2013, **4**, 1369-1-7.
9 W. Bryks, M. Wette, N. Velez, S. W. Hsu and A. R. Tao, *J. Am. Chem. Soc.*, 2014, **136**, 6175-6178.
10 W. P. Lim, C. T. Wong, S. L. Ang, H. Y. Low and W. S. Chin, *Chem. Mater.*, 2006, **18**, 6170-6177.
11 H. Lee, S. W. Yoon, E. J. Kim and J. Park, *Nano Lett.*, 2007, **7**, 778-784.
12 L. R. Guo, D. D. Yan, D. F. Yang, Y. J. Li, X. D. Wang, O. Zalewski, B. F. Yan and W. Lu, *ACS Nano*, 2014, **8**, 5670-5681.
13 E. Thimsen, U. R. Kortshagen and E. S. Aydil, *Chem. Commun.*, 2014, **50**, 8346-8349.
14 W. Han, L. Yi, N. Zhao, A. Tang, M. Gao and Z. Tang, *J. Am. Chem. Soc.*, 2008, **130**, 13152-13161.
15 P. Nørby, S. Johnsen and B. B. Iversen, *ACS Nano*, 2014, **8**, 4295-4303.
16 Y. Wu, C. Wadia, W. Ma, B. Sadtler and A. P. Alivisatos, *Nano Lett.*, 2008, **8**, 2551-2555.
17 D. Mott, J. Yin, M. Engelhard, R. Loukrakpam, P. Chang, G. Miller, I. T. Bae, N. Chandra Das, C. Wang, J. Luo and C. J. Zhong, *Chem. Mater.*, 2010, **22**, 261-271.
18 Z. Zhuang, X. Lu, Q. Peng and Y. Li, *Chem. Eur. J.*, 2011, **17**, 10445-10452.
19 W. Aigner, G. K. Nenova, M. A. Sliem, R. A. Fischer, M. Stutzmann and R. N. Pereira, *J. Phys. Chem. C*, 2015, **119**, 16276-16285.
20 M. Kruszynska, H. Borchert, A. Bachmatiuk, M. H. Rümmeli, B. Büchner, J. Parisi and J. Kolny-Olesiak, *ACS Nano*, 2012, **6**, 5889-5896.
21 M. Kanehara, H. Arakawa, T. Honda, M. Saruyama and T.Teranishi, *Chem. Eur. J.*, 2012, **18**, 9230-9238.
22 Y. Zhang, X. Li, W. Xu, S. Li, H. Wang and L. S. Li, *Mater. Lett.*, 2012, **67**, 117-120.
23 X. L. Wang, Y. J. Ke, H. Y. Pan, K. Ma, Q. Q. Xiao, D. Q. Yin, G. Wu and M. T. Swihart, *ACS Catal.*, 2015, **5**, 2534-2540.
24 S. D. Sun, S. Wang, D. C. Deng and Z. M. Yang, *New J. Chem.*, 2013, **37**, 3679-3684.
25 M. Lotfipour, T. Machani, D. P. Rossi and K. E. Plass, *Chem. Mater.*, 2011, **23**, 3032-3038.

26 A. Putnis, *Philos. Mag.*, 1976, **34**, 1083-1086.
27 G. Donnay, J. D. H. Donnay and G. Kullerud, *Am. Mineral.*, 1958, **43**, 228-242.
28 B. Mulder, *J. Phys. Stat. Sol. (a)*, 1972, **13**, 79-88.
29 S. K.Haram, A. R. Mahadeshwar and S. G. Dixit, *J. Phys. Chem.*, 1996, **100**, 5868-5873.
30 K. Koto and N. Morimoto, *Acta Cryst. B*, 1970, **26**, 915-924.
31 H. Nozaki, K. Shibata and N. Ohhashi, *J. Solid State Chem.*, 1991, **91**, 306-311.
32 W. Liang and M. H. Whangbo, *Solid State Commun.*, 1993, **85**, 405-408.
33 M. Leon and N. Terao, *Phys. Status Solidi A*, 1981, **67**, K11-K14.
34 M. M. Kazinets, I. V. Ivanova and R. B. Shafizade, *Phase Trans.*, 1979, 1, 199-206.
35 S. Wang, *Mater. Chem. Phys.*, 2002, **75**, 32-38.
36 X. C. Jiang, Y. Xie, J. Lu, W. He, L. Y. Zhu and Y. T. Qian, *J. Mater. Chem.*, 2000, **10**, 2193-2196.
37 Y. B. Chen, L. Chen and L. M. Wu, *Cryst. Growth & Des.*, 2008, **8**, 2736-2740.
38 C. Y. Wang, Z. Fang, F. Fan, X. N. Dong, Y. Peng, S. H. Hao and L. Y. Long, *CrystEngComm*, 2013, **15**, 5792-5798.
39 H. M. Zheng, J. B. Rivest, T. A. Miller, B. Sadtler, A. Lindenberg, M. F. Toney, L. W. Wang, C. Kisielowski and A. P. Alivisatos, *Science*, 2011, **333**, 206-209.
40 J. B. Rivest, L. K. Fong, P. K. Jain, M. F. Toney and A. P. Alivisatos, *J. Phys. Chem. Lett.*, 2011, **2**, 2402-2406.
41 L. G. Liu, H. Z. Zhong, Z. L. Bai, T. Zhang, W. P. Fu, L. J. Shi, H. Y. Xie, L. G. Deng and B. S. Zou, *Chem. Mater.*, 2013, **25**, 4828-4834.
42 Q. W. Tian, M. H. Tang, Y. G. Sun, R. J. Zou, Z. G. Chen, M. F. Zhu, S. P. Yang, J. L. Wang, J. H. Wang and J. Q. Hu, *Adv. Mater.*, 2011, **23**, 3542-3547.
43 Y. Xie, A. Riedinger, M. Prato, A. Casu, A. Genovese, P. Guardia, S. Sottni, C. Sangregorio, K. Miszta, S. Ghosh, T. Pellegrino and L. Manna, *J. Am. Chem. Soc.*, 2013, **135**, 17630-17637.
44 Y. Xie, L. Carbone, C. Nobile, V. Grillo, S. D'Agostino, F. Della Sala, C. Giannini, D. Altamura, C. Oelsner, C. Kryschi and P. D. Cozzoli, *ACS Nano*, 2013, **7**, 7352-7369.
45 Q. W. Tian, F. R. Jiang, R. J. Zou, Q. Liu, Z. G. Chen, M. F. Zhu, S. P. Yang, J. L. Wang, J. H. Wang and J. Q. Hu, *ACS Nano*, 2011, **5**, 9761-9771.
46 B. Li, Q. Wang, R. J. Zou, X. J. Liu, K. B. Xu, W. Y. Li and J. Q. Hu, *Nanoscale*, 2014, **6**, 3274-3282.
47 H. Fjellvag, F. Grønvold, S. Stølen, A. F. Andresen, R. Müller-Kafer and A. Simon, *Z. Kristallogr.*, 1988, **184**, 111-121.
48 M. Grioni, J. B. Goedkoop, R. Schoorl, F. M. F. de Groot, J. C. Fuggle, F. Schafers, E. E. Koch, G. Rossi, J. M. Esteva and R. C. Karnatak, *Phys. Rev. B*, 1989, **39**, 1541-1545.
49 P. Kumar, R. Nagarajan and R. Sarangi, *J. Mater. Chem. C*, 2013, **1**, 2448-2454.
50 I. I. Mazin, *Phys. Rev. B*, 2012, **85**, 115133-1-8.
51 S. Pande, S. Jana, S. Basu, A. K. Sinha, A. Datta and T. Pal, *J. Phys. Chem. C*, 2008, **112**, 3619-3626.
52 G. Liu, X. Mu, H. Zhang and P. Chen, *Chem. Sci.*, 2014, **5**, 275-280.
53 Y. C. Jiang, S. D. Zhang, Q. Ji, J. Zhang, Z. P. Zhang and Z. Y. Wang, *J. Mater. Chem. A*, 2014, **2**, 4574-4579.
54 A. Putnis, *Am. Mineral.*, 1977, **62**, 107-114.

Graphical abstract